LST-1, the Large-Sized Telescope prototype of CTA. Status and first observations.

Abelardo Moralejo[1] **for the CTA-LST project**

[1]Institut de Fisica d'Altes Energies (IFAE), The Barcelona Institute of Science and Technology, Campus UAB, 08193 Bellaterra (Barcelona), Spain.

E-mail: `moralejo@ifae.es`

Abstract. CTA (Cherenkov Telescope Array) is the next generation ground-based observatory for gamma-ray astronomy at very-high energies. Once completed, CTA will outperform present-day facilities by an order of magnitude in sensitivity, and significantly enlarge the accessible energy range and survey capabilities. Deployed in the CTA north site, on the island of La Palma (Spain), LST-1 is the prototype for the CTA Large-Sized Telescopes, which will cover the lower end of the energy range of the array, down to 20 GeV. LST-1 started astronomical observations in late 2019, and is currently completing its commissioning phase. We present the status of the instrument and an overview of the first physics results.

1. Introduction

The Large-Sized Telescope (LST) project for CTA has been developed by a collaboration of more than 300 scientists and engineers from about 30 institutes in 12 countries: Brazil, Bulgaria, Czech Republic, Croatia, France, Germany, India, Italy, Japan, Poland, Spain, and Switzerland. With a focus on the lower-energy end of CTA (down to 20 GeV), the LSTs feature a lightweight structure and fast slewing capabilities to allow the follow-up of short transient phenomena in the very-high-energy (VHE) band. LST-1, the prototype LST, was built and deployed at the *Roque de los Muchachos* observatory, on the Canary island of La Palma, between 2016 and 2018, and is currently completing its commissioning phase. Figure 1 shows a picture of the telescope and a summary of its main elements: the supporting structure with an alt-azimuthal mount, a 23-m diameter parabolic mirror dish, and a 4.5°-field-of-view camera equipped with 1855 photomultipliers (PMTs) and fast (GHz) readout electronics.

The physics program of the LSTs, and of the whole CTA project [1], is mostly concerned with the study of particle acceleration in extreme astrophysical environments in our galaxy and beyond (e.g. supernova remnants, super-massive black holes), and with fundamental physics topics for which VHE photons are potentially key probes, like indirect dark matter searches, or tests of possible violations of the Lorentz invariance.

2. Data acquisition and processing

LST-1 collects the Cherenkov light from the extensive air showers of particles initiated by VHE photons or charged cosmic rays (the latter being much more abundant). Depending on the observation conditions, between 6×10^3 and 10×10^3 showers are recorded every second. For

Journal of Physics: Conference Series **2156** (2022) 012089 doi:10.1088/1742-6596/2156/1/012089

Optics	
Optics layout	Parabolic mirror
Primary mirror diameter (m)	23
Secondary mirror diameter (m)	–
Eff. mirror area after shadowing (m^2)	368
Focal length (m)	28
Focal plane instrumentation	
Photo sensor	PMT
Pixel size (degr.), shape	0.10, hex.
Field of view (degr.)	4.5
Number of pixels	1855
Signal sampling rate	GHz
Structure	
Mount	alz-az, on circular rail
Structural material	CFRP / steel
Weight (full telescope, tons)	100
Max. time for repositioning (s)	20

Figure 1. LST-1 in the *Roque de los Muchachos* observatory on the island of La Palma.

each event the signals from all the PMTs are digitized, resulting in 40 1-ns-long samples per pixel stored on disk for subsequent analysis.

The analysis of the LST-1 data is performed using `cta-lstchain`[1], a pipeline based on `ctapipe`[2], the framework for prototyping the low-level data processing algorithms for CTA. The first step is the camera calibration [4], to convert the digitized samples into physical units (photo-electrons). In Fig. 2, the total integrated charge (in photo-electrons per pixel) is shown for three different types of events. The events triggered by single muons, like the one in Fig. 2(c), can be used to calibrate the total light throughput of the telescope and the last part of the atmosphere (Fig. 3(a)), since the total Cherenkov photon yield is easily predictable [3]. The light intensity profile along the ring radius (Fig. 3(b)) also provides a validation of the optical point-spread function of the telescope.

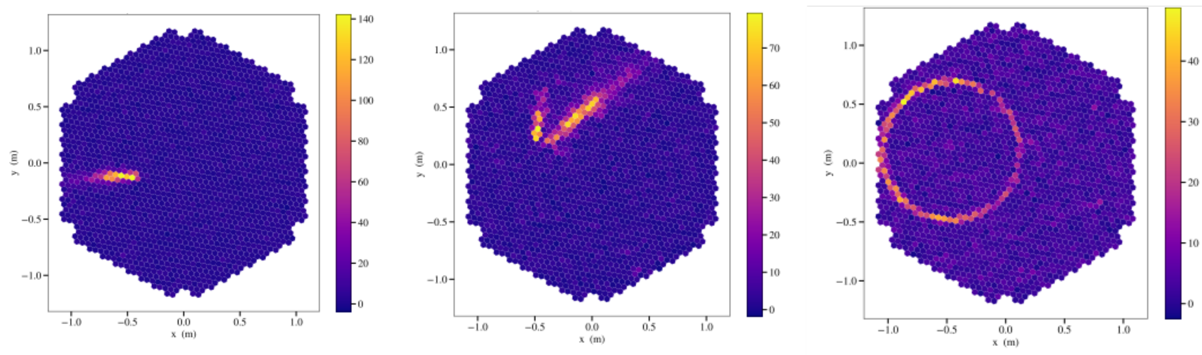

(a) (b) (c)

Figure 2. Different types of images recorded by LST-1 during an observation. (a): A gamma-ray candidate; (b): a shower with two electromagnetic sub-showers, most likely initiated by a cosmic-ray proton; (c) a muon ring, produced by a muon going through the telescope mirror.

The analysis of shower events, which comprise the majority of the LST-1 triggers, starts with an image cleaning procedure which selects pixels with signals dominated by Cherenkov light

[1] https://github.com/cta-observatory/cta-lstchain
[2] https://github.com/cta-observatory/ctapipe

Journal of Physics: Conference Series **2156** (2022) 012089 doi:10.1088/1742-6596/2156/1/012089

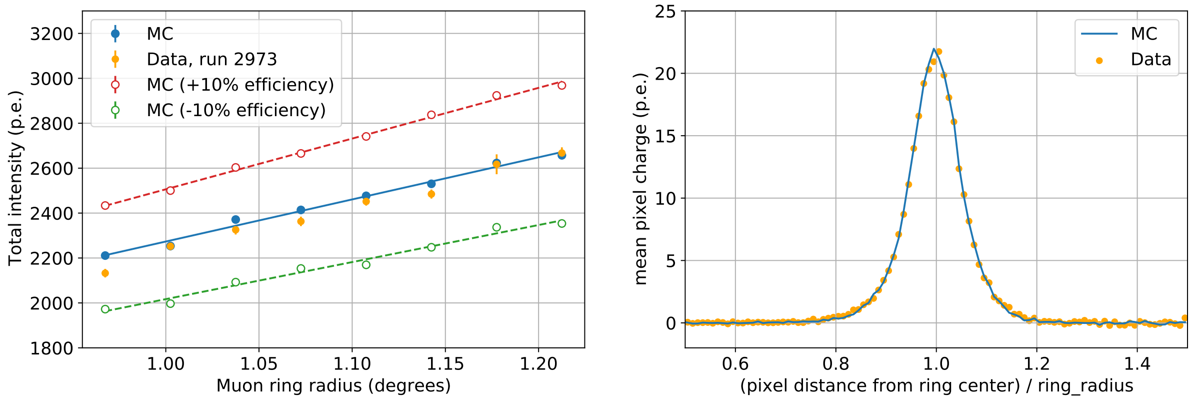

(a) (b)

Figure 3. (a): Total light in muon rings detected by LST-1 vs. ring radius. Data from one run is compared to three different simulations, with telescope efficiency changing in steps of 10%. (b): average radial charge profile of muon rings, in units of the ring radius.

from the recorded shower, rather than by background light from the night sky. The resulting clean image is then characterized by a set of simple parameters, including the moments of the light distribution of the images, going up to 3^{rd} order. The calibrated and parametrized images constitute the Data Level 1 (DL1).

We use Random Forests [5], with image parameters as inputs, and trained on Monte Carlo (MC) simulations [6] to select γ-ray candidates among the overwhelming background of hadron-initiated showers, and to estimate the arrival direction and the energy of the primary gamma rays. These Random Forests are applied to the DL1 data; the output of this stage, the DL2 data level, consists of event lists containing the reconstructed shower parameters: energy, direction and *gammaness*, a score in the range 0 to 1, ranging from least- to most-gamma-like, which allows us to select samples of gamma-like events with different levels of residual background. Figure 4 shows the LST-1 performance in terms of angular and energy resolution, as a function of gamma-ray energy. A slightly more sensitive analysis (the so-called source-dependent approach) can be performed for point-like gamma-ray sources of known location. The *a priori* knowledge of the gamma-ray directions provides a better reconstruction of the shower impact parameter,

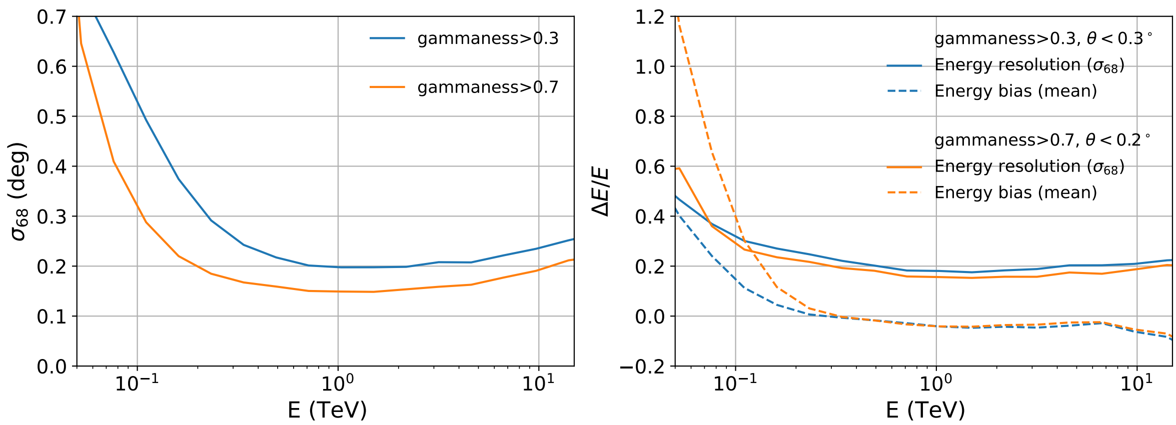

Figure 4. Angular and spectral resolutions of LST-1 versus true energy obtained with MC simulations. Two different values of the gamma-ray selection cut are shown. θ is the angle between the reconstructed direction and the observed source.

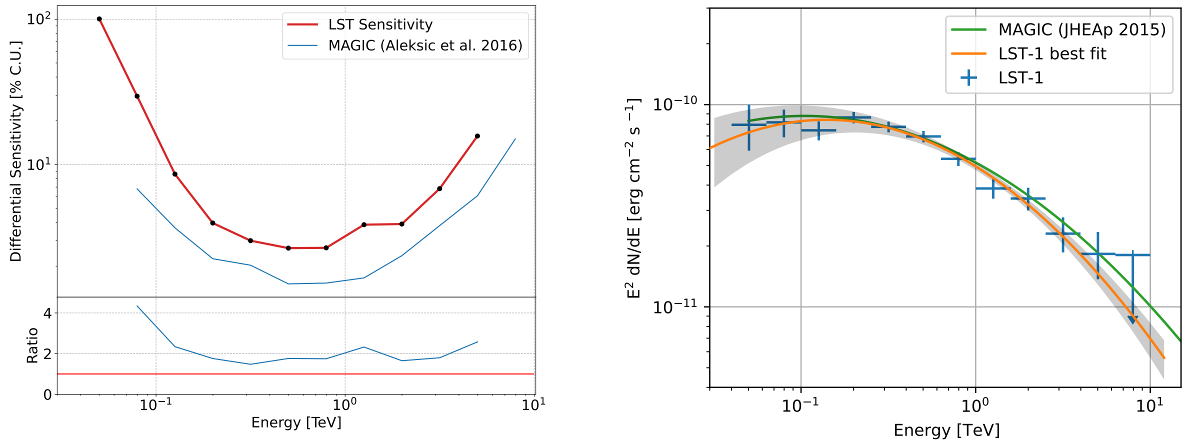

(*a*) (*b*)

Figure 5. (*a*): LST-1 differential sensitivity in 50 hours of observation of a point-like source, compared to that of MAGIC. (*b*): SED of the Crab Nebula as determined with LST-1 in a 3.5-h observation, compared to the MAGIC best-fit SED from [7].

hence of the gamma-ray energy and of the identity of the primary. Figure 5(*a*) shows the LST-1 sensitivity[3] for point-like sources using the source-dependent analysis, determined from observations of the Crab Nebula. Note that, as a single Cherenkov telescope, LST-1 does not yet outperform existing *stereoscopic* facilities like MAGIC in the overlapping energy range.

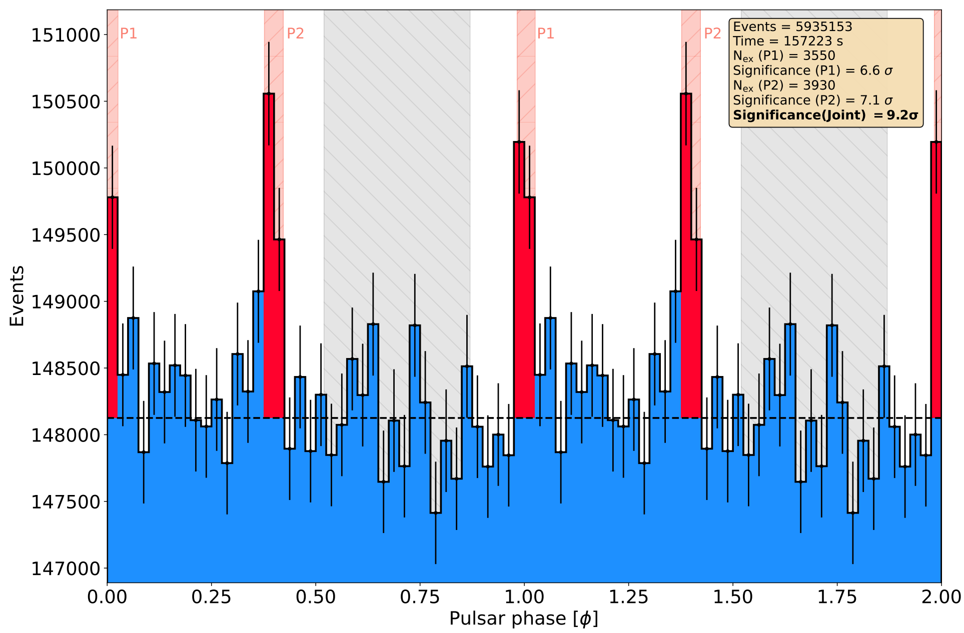

Figure 6. Phaseogram of the Crab pulsar, obtained with 43.7 hours of observation with LST-1. Phase range definitions taken from [8].

3. Early physics results

The Crab Nebula, the standard candle of gamma-ray astronomy, has been regularly observed during the LST-1 commissioning. Fig. 5(*b*) shows the Spectral Energy Distribution (SED)

[3] as defined in https://www.cta-observatory.org/science/cta-performance/

obtained with 3.5 hours of LST-1 observations of the source on the night of the 20th of November 2020 (a so-called *reference night*, with good weather conditions and overall performance of the telescope). The SED is compatible with measurements by MAGIC and other VHE observatories. The VHE pulsation from PSR J0534+220, the pulsar at the center of the nebula, is also clearly visible in 43.7 hours of data collected between January 2020 and March 2021 (see Fig. 6)

Beyond our own galaxy, the VHE sky is dominated by blazars, active galactic nuclei with a jet closely aligned to the line of sight. During its commissioning phase, LST-1 has observed and successfully detected five blazars: Mrk 501, Mrk 421, 1ES 1959+650, 1ES 0647+250 and PG 1553+113. Figure 7 shows the results for one observation of Mrk 421.

4. Conclusions and Outlook

The CTA LST-1 telescope is close to completing its commissioning phase, and gradually moving into scientific exploitation. Despite the comparatively modest performance attainable by a standalone atmospheric Cherenkov telescope (with respect to stereoscopic arrays), several known sources have been successfully detected by LST-1. The completion of the 4-LST stereoscopic array in the CTA-N observatory, expected by late 2024, will bring CTA to its design performance below 200 GeV, significantly outperforming existing facilities in this energy range.

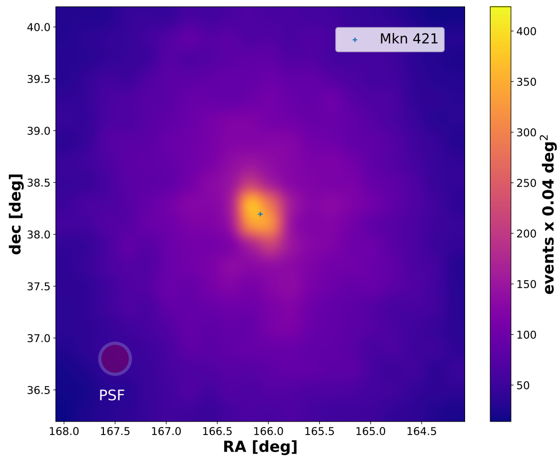

(*a*)

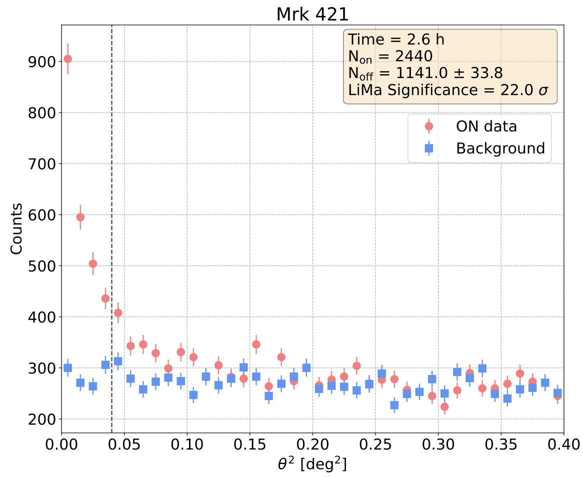

(*b*)

Figure 7. (*a*): Smoothed sky map of gamma-like events recorded around the active galaxy Mrk 421. (*b*): Distribution of the squared angular distances between the reconstructed event directions and the nominal source position.

Acknowledgements

We gratefully acknowledge financial support from the agencies and organizations listed here: http://www.cta- observatory.org/consortium_acknowledgments.

References

[1] Acharyya, A *et al* (The CTA Consortium) 2017 *Science with the Cherenkov Telescope Array* https://arxiv.org/abs/1709.07997
[2] Mazin D *et al* 2021 *Proceedings of 37th ICRC* https://doi.org/10.22323/1.395.0872
[3] Gaug M *et al* 2019 ApJS **243** 42
[4] Kobayashi Y *et al* 2021 *Proceedings of 37th ICRC* https://doi.org/10.22323/1.395.0720
[5] Breiman L 2001 *Machine Learning* **45** 5
[6] Acharyya A *et al* 2019 *Astroparticle Physics* **111** 35
[7] Aleksić J *et al* (MAGIC collaboration) 2015 *JHEAp* **5**
[8] Aleksić J *et al* (MAGIC collaboration) 2012 *A&A* **540** A69